

## Structural, Potential Surface and Vibrational Spectroscopy Studies of Hypophosphorous Acid in the Gas Phase and Chain Conformation. A Theoretical Study

I. Ahmadi, H. Rahemi\* and S.F. Tayyari†

Chemistry Department, Urmia University, Urmia, 57159-165 Iran

\*Chemistry Department, Ferdowsi University, Mashhad, 91775-1435 Iran

(2004. 11. 10 접수)

## Structural, Potential Surface and Vibrational Spectroscopy Studies of Hypophosphorous Acid in the Gas Phase and Chain Conformation. A Theoretical Study

I. Ahmadi, H. Rahemi\* and S.F. Tayyari†

Chemistry Department, Urmia University, Urmia, 57159-165, Iran

†Chemistry Department, Ferdowsi University, Mashhad, 91775-1435, Iran

(Received November 10, 2004)

**요약.** Hypophosphorous acid (HPA) 분자의 구조와 진동 위치에너지 표면을 HF, MP2, DFT-B3LYP 등의 이론적인 계산 방법을 이용하여 연구하였다. HPA 분자의 체인 수를 증가시켰을 때, 계산된 진동 frequency가 실험값에 보다 근접하게 되는 현상을 관측하였다. P-O 결합에 수직인 O=P-O-H 각도의 함수로 나타낸 위치에너지 표면은 O=P-O 평면의  $\pm 42.5^\circ$ 에서 최소 에너지를 나타내며, saddle point와 복잡한 형태의 에너지 장벽을 보여준다. P-O-H의 비평면 진동운동에 대한 위치에너지 함수에 따르면 전자 바닥 함수에서는  $284.87\text{ cm}^{-1}$ 의 위치에너지 장벽을 보여주지만, 전자 들뜬 상태에서는 위치에너지 장벽이 나타나지 않았다.

**주제어:** DFT; IR, VCD, Vibrational Spectra, Isomeric Pathway, Hypo Phosphorous Acid

**ABSTRACT.** The potential energy surfaces (PES), molecular and vibrational structure of hypophosphorous acid (HPA) were investigated by HF, MP2 and DFT-B3LYP level of theory using 6-31G\*\* basis set. In order to approach solid state spectra we optimized mono-, di-, tri-, tetra- and penta-mer structures and computed frequencies and intensities of the vibrational modes of VCD and IR. It is found that by increasing the number of HPA molecules in the chain, some of calculated vibrational frequencies approach to the experimental solid state values. The potential energy surfaces of HPA are calculated in a wide range on the plane perpendicular to the P-O bond where the hydrogen can rotate 360 degree through O=P-O-H dihedral angle. A circular valley is found going up and down on the plane, the valley is centered to the continuation of P-O bond. There are two minima at angles  $\pm 42.5^\circ$  to the O=P-O plane giving two mirror conformers and one saddle point in between with a height of  $284.87\text{ cm}^{-1}$  at the angles  $0^\circ$  and a complex barrier with a height of  $2089.40\text{ cm}^{-1}$  at the angle  $180^\circ$  to the same plane. On top of the complex barrier, there is a small well with depth of  $15.65\text{ cm}^{-1}$ . To study the tunneling effect and pathway between the two conformers, the molecule is considered to have  $C_s$  symmetry and a symmetric double minimum potential energy well with a barrier of  $284.87\text{ cm}^{-1}$  height in the middle. With the constructed potential, the torsional motion of P-O-H (Hindered Rotation) of the monomer, using variation method and harmonic oscillator wave functions is studied and IR frequencies and relative intensities of vibrational modes are calculated. Due to the width of the well and the trigonometric shape of the barrier, tunneling can occur at the ground state

and the next excited state does not feel the barrier at all.

**Keywords:** DFT; IR, VCD, Vibrational Spectra, Isomeric Pathway, Hypo Phosphorous Acid

## INTRODUCTION

In spite of extensive experimental studies of molecules containing phosphate moieties,<sup>1</sup> only sporadic data exist for small organophosphates. In addition, few theoretical studies, most of which involve low-level calculations with small basis sets, are available for these molecules.

Ab initio calculations usually are carried out in order to obtain conformational, vibrational and other molecular information for a set of small oxygen-containing phosphorus compounds. Many of these molecules are fundamentally important since they are analogous to macrostructures that play a central role in biological processes. It is anticipated that the chemical and physical properties of these phosphorus compounds will provide valuable insight into problems in structural biology.<sup>2</sup> In the present work, our attention will be focused on the conformational and vibrational analyses of HPA and its deuterated analogous in the gas phase.

The structure of HPA crystals features chain association of the acid molecules connected by very short hydrogen bonds with symmetric potential wells. Diffraction work<sup>3</sup> has left the problem of the "true" symmetry of these bonds. Previous IR investigations of HPA were handicapped by the lack of both crystal structure data and experience with very short hydrogen bonds.<sup>4-7</sup>

Crystalline structure of HPA is determined by diffraction method,<sup>8</sup> it is orthorhombic with space symmetry group  $P2_12_12$  or  $D_2^3(z-2)$  with melting point 26.5°C. The molecule aggregates in zig-zag chains through hydrogen bonds. The O...O dis-

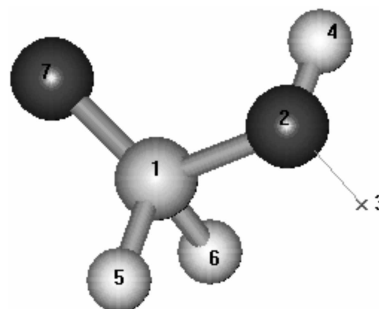


Fig. 1. Optimized structure of the  $H_3PO_2$  molecule with Gaussian and displayed by Hyperchem. Atom No 1 is the Phosphorus atom, dark colored atoms are Oxygen atoms and white colored atoms are Hydrogen atom.

tance is 2.44 Å parallel to the crystallographic  $z$  axis. The symmetry of a single molecule in the lattice is  $C_1$ , Fig. 1. The HPA molecules have only one hydrogen atom bonded to oxygen thus it is a mono protonic oxy acid. This compound is a weak acid and forms only one series of hypophosphate salts.<sup>9</sup> In the liquid state, it is expected that chains of molecules resume their structures as a polymer, Fig. 2. Unfortunately, in the gas phase the molecule is unstable and regroups to phosphoric acid and phosphorus tri hydrogen, therefore, its IR and Raman spectra have not been reported.<sup>2</sup>

## COMPUTATIONAL METHOD

The ab initio calculations were carried out with the GAUSSIAN 98W A.6 system of program.<sup>10</sup> Full geometry optimizations were done at the HF/6-31G\*\*,<sup>11</sup> MP2/6-31G\*\*,<sup>12</sup> and B3LYP/6-31G\*\*<sup>13</sup> levels of theory. The theoretical harmonic vibrational fre-

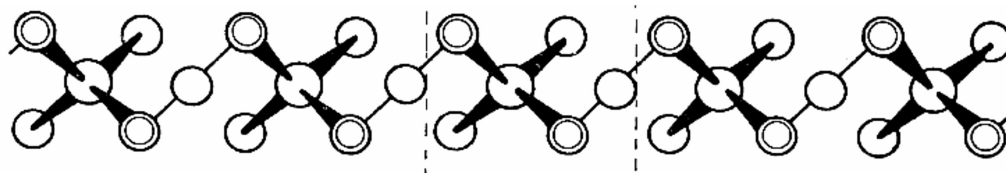


Fig. 2. Proposed liquid state chain conformation of HPA.

quencies and IR and VCD intensities were also calculated analytically at the same levels.

In order to approach the solid state IR spectra, conformations of one-, two-, three-, four- and five-molecules in a chain were optimized using B3LYP/6-31G\*\*.

To obtain the potential surfaces a plane perpendicular to P-O bond is chosen and the hydrogen atom in an area of 2.6×2.6 Å by step of 0.1 Å is scanned. Next the O-H bond was rotated about P-O direction so the H-O-P=O dihedral angle was changed from 0° to 360° and scanned by step of 1° while all other structural parameters kept constant at their equilibrium position. From which double minimum potential energy profile is constructed. Finally the O-H bond is scanned from 0.1 to 1.7 Å by step of 0.01 Å.

## RESULTS AND DISCUSSION

### A. HPA (Monomer)

The defined bond angles and bond lengths of the HPA are shown in Fig. 1. The optimized structural parameters of single molecule calculated by different theoretical approaches are listed in Table 1.

In spite of the calculated free HPA geometry parameters are compared to the solid state HPA results; the parameters at MP2/6-31G\*\* and B3LYP/6-31G\*\* levels are close to the each other values while those obtained at HF/6-31G\*\* level are a little different. For example the calculated O-H bond length for a free HPA at B3LYP, MP2, and HF lev-

els are 0.9689, 0.9671, 0.947 Å, respectively.

Frequency assignments are done by animating vibrational modes using Gauss View2.1 and Hyper Chem7.<sup>14</sup> Inspection of Table 2 shows that calculated frequencies obtained by B3LYP and MP2 levels are in good agreement with the experimental data but markedly different from those obtained by HF approach and demonstrating the effect of electron correlation corrections. The calculated values by MP2 at low frequencies and B3LYP at high frequencies are more close to the experimental values. However, it must be pointed out that in Table 2 gas phase frequencies are compared to those of solid state.

The IR absorption spectrum of the acid and its deuterated analogous are constructed from calculated intensities and fixed full bandwidth of 20 cm<sup>-1</sup> and presented in the Fig. 3a and Fig. 3c using Gaussian band shape functions.

The optical activity of dissymmetric molecules is explained when a plane polarized radiation passes through an active medium. The plane of the emergent plane polarized radiation rotates by an angle. The plane polarized beam can be considered as a superposition of two oppositely rotating circularly polarized component. The absorbance coefficient is defined<sup>15</sup>  $\Delta\epsilon = \epsilon_L - \epsilon_R$  and the line shape is nearly Gaussian. The absorbance coefficient of the VCD is given by

$$\Delta\epsilon = \frac{2\sqrt{\ln 2} R \bar{\nu}}{2.296 \times 10^{-39} \sqrt{\pi} \Gamma_{1/2}} \exp \left[ 4 \ln(2) \left( \frac{\bar{\nu} - \bar{\nu}_0}{\Gamma_{1/2}} \right)^2 \right] \quad (1)$$

Table 1. The optimized geometrical parameters of the HPA (in Angstroms and Degrees)

Expt. Solid <sup>18</sup>	HF/6-31G**	MP2/6-31G**	B3LYP/6-31G**	Structural Parameter
1.512	1.596	1.628	1.628	R(P-O)
1.392	1.388	1.399	1.416	R(P-H)
1.392	1.388	1.393	1.410	R(P-II)
1.512	1.457	1.488	1.485	R(P=O)
1.22	0.947	0.967	0.969	R(O-II)
-	102.0	103.4	103.7	∠(II-P-O)
-	102.0	96.8	97.0	∠(II-P-O)
114.9	115.4	118.2	117.9	∠(O=P-O)
106.3	103.5	103.7	103.6	∠(II-P-II)
-	115.9	118.0	117.9	∠(II-P=O)
-	113.1	111.9	111.9	∠(P-O-II)

Table 2. Assignments of the calculated frequencies ( $\text{cm}^{-1}$ ) of the HPA and HPA<sub>d</sub> with used methods and comparison of them with the solid state spectra

HPA <sub>d</sub>				HPA		Assignment
Expt.[8]	B3LYP/6-31G**	Expt.[8]	B3LYP/6-31G**	MP2/6-31G**	HF/6-31G**	
238	182.6	232	237.5	238.1	83.7	OPOH torsion
-	385.6	394	413.3	422.4	408.2	OP (OH)bend+OH torsion
635	610.3	805	785.1	811.0	910.5	PH <sub>2</sub> rock+POH bend
982	661.0	1015	859.7	878.7	958.7	P-(OH) stretch
765	777.2	928	898.2	935.1	990.0	PH <sub>2</sub> twist
1145	805.5	1130	1028.1	1049.7	1071.1	POH bend-HPO bend
718	860.2	1098	1117.1	1162.0	1243.3	PH <sub>2</sub> wag+POH bend
805	872.9	1122	1165.0	1212.8	1296.6	PH <sub>2</sub> scissor-P=O stretch
930	1271.6	1260	1296.6	1327.9	1408.4	PH <sub>2</sub> scissor+P=H stretch
1772	1745.9	2442	2427.1	2562.2	2670.7	PH asymm. stretch
1798	1780.5	2465	2474.2	2611.3	2690.1	PH sym. stretch
1100	2777.1	1100	3817.1	3888.3	4157.5	OH stretch

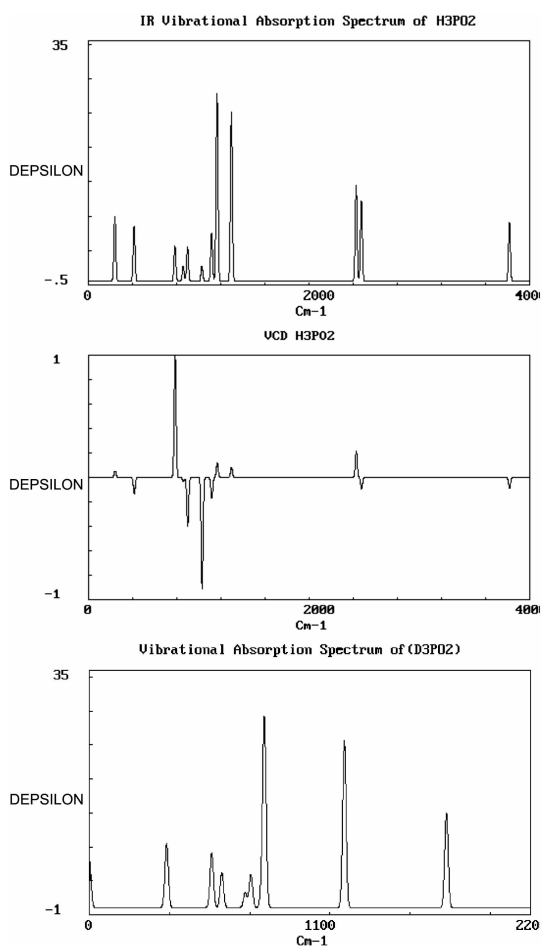


Fig. 3. a- IR, b- VCD and c- deuterated absorption spectrum of the H<sub>3</sub>PO<sub>2</sub>.

Where R is the rotational strength and  $\Gamma_{1/2}$  is the full width at the half height. Using the full line width 20  $\text{cm}^{-1}$  similar to IR absorbance spectra, the VCD spectra are shown in Fig. 3b. As shown in Fig. 3b PH<sub>2</sub> rock ( $\nu$ -784  $\text{cm}^{-1}$ ) is strongly left polarized and PH<sub>2</sub> twist ( $\nu$ -898  $\text{cm}^{-1}$ ) is strong right polarized.

To obtain the potential surfaces a plane perpendicular to P-O bond is chosen and the hydrogen atom in an area of  $2.6 \times 2.6 \text{ \AA}$  by step of 0.1  $\text{\AA}$  is scanned. Three presentations which are prepared by using Surfer<sup>10</sup> soft ware are shown in Figs. (4 and 5). All of the numerical values of the potential energy of scanned area are inspected and a valley found whose deepest points going up and down on the

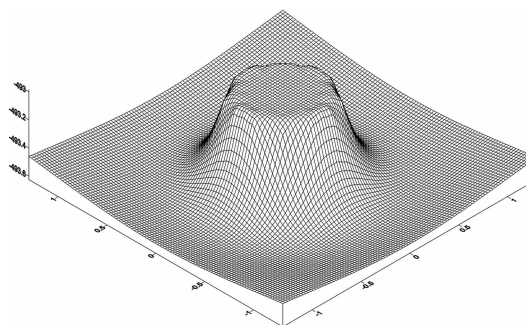


Fig.4. The truncated and net presentation of the PES displayed by Surfer. The O=P-O plane is perpendicular and crossing through right hand side O. From (-1, -1) corner the minimum can be clearly detected.

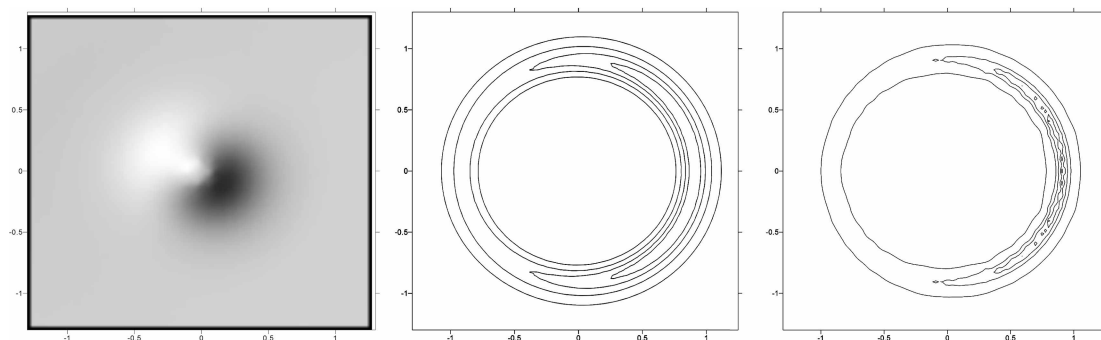


Fig. 5. a- the smooth and complete surface presentation, b and c- contour (iso-potential) map presentations of the PES displayed by Surfer.

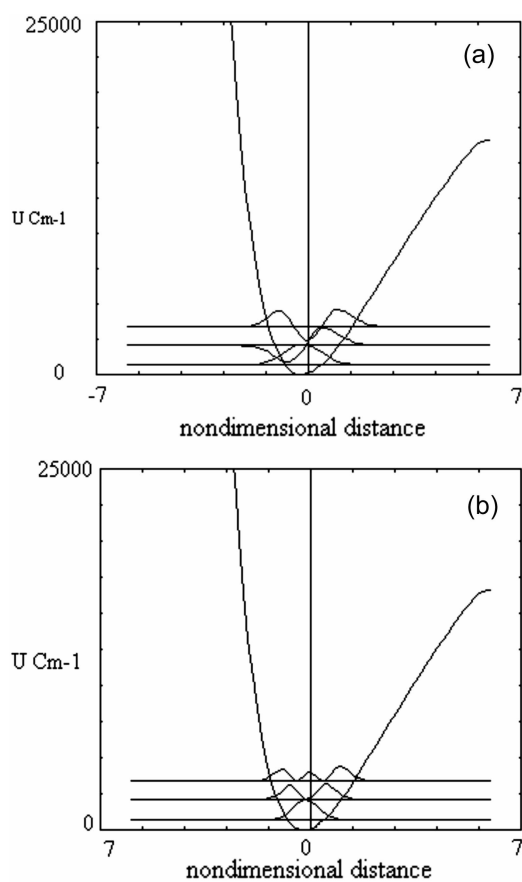


Fig. 6. The OH potential energy and a few vibrational energy levels: (a) wave functions and (b) probability distributions.

locations of hydrogen atom if O-H bond precess, Fig. 5b. In another and more involved scan, the O-H precession is carried out and isomeric pathway, double minimum potential energy, is gener-

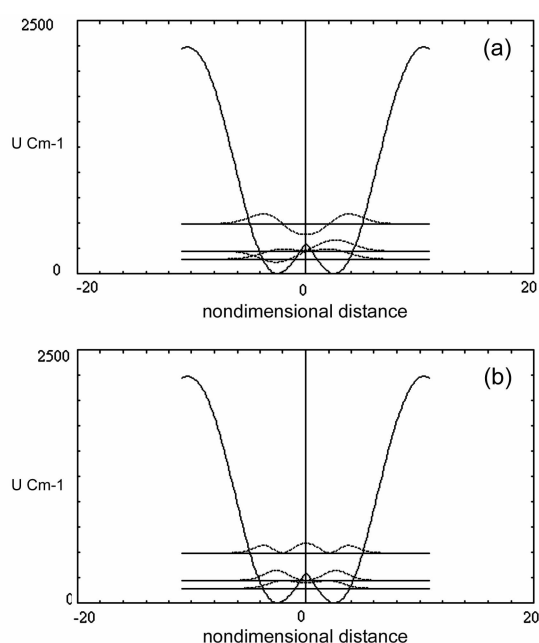


Fig. 7. Spatial isomeric pathway, barrier height and tunneling effect between them a: energy levels and wave functions, b: energy levels and probabilities distributions.

ated and opened up for tunneling studies, Fig. 7. There are two minima at  $\pm 42.5^\circ$  and a saddle point in between ( $0^\circ$ ) with a height of  $284.87 \text{ cm}^{-1}$  and a complex barrier at  $180^\circ$  with the  $2089.40 \text{ cm}^{-1}$  height to the O=P-O plane. On the top of the complex barrier, there is a small well with the depth  $15.65 \text{ cm}^{-1}$ .

The free O-H stretch ( $C_1$ , to check our own generated computer program) and P-O-H torsion ( $C_3$ ) of the IIPA can be seen in the gas phase spectrum of the acid if it would be available, unfortunately

the acid in gas phase immediately disintegrate to  $\text{PH}_3$  and  $\text{H}_3\text{PO}_4$ . Therefore, the gas phase spectrum has not been reported.<sup>3</sup> The dynamics of a microscopic particle such as stretching can be appropriately described with one-dimensional Schrödinger Equation.<sup>17</sup>

For the present case  $V(R)$  of the stretching vibrational mode, which is produced by scanning the O-H bond length from 0.1 Å-1.75 Å and for the spatial isomeric pathway potential (torsional motion) a scanning of the torsional angle 360° with fixed bond length and using the Gaussian 98 computer program, Figs. 6 and 7. Wide double well potential curve of the pathway with a sharp and small barrier resulted. The net effect would be lowering the torsional frequency.

Introducing the dimensionless variable<sup>17</sup>  $\xi = (\mu\omega/\eta)^{1/2}R$  to the Schrödinger Equation and by using the variation method and harmonic oscillator wave functions as basis sets:

$$\Psi(\xi) = \sum_{i=0}^{\infty} C_i G_i(\xi) \quad (2)$$

We define matrix elements  $H_{jk}$ , as:

$$H_{jk} = HK_{jk} + HU_{jk} \quad (3)$$

Where

$$HK_{jk} = \int \Phi_j^*(\xi) \frac{d^2}{d\xi^2} \Phi_k(\xi) d\xi$$

$$HU_{jk} = \int \Phi_j^*(\xi) \frac{2\mu V(R)}{\eta \omega_s} \Phi_k(\xi) d\xi \quad (4)$$

The matrix elements  $HK_{jk}$  and  $HU_{jk}$  are computed analytically and numerically respectively. By using Eq. (2) wave functions are generated and after computational performances the results of the both computations for three energy levels and wave functions are reflected in Figs. 6 and 7.

As it is clear from the Fig. 7: due to the width (minima to minima 85°, about 2.0 Å) and height (284.87  $\text{cm}^{-1}$ ) of the well and also to the trigonometric shape of the barrier, tunneling occurred at the ground state and the next vibrational excited state does not felt the barrier at all. Therefore conformational transition energy is not required.

#### B. two, three, four and five unit chain of the HPA

Vibrational spectra of crystalline HPA and its deuterated analogous have been studied with both IR and Raman techniques.<sup>8</sup> The structural optimization of two, three, four and five molecules in chains are performed using DFT with B3LYP/6-31G\*\* level. The optimized structures Fig. 8(a, b, c, d) clearly show that the chain in free space is screwing.

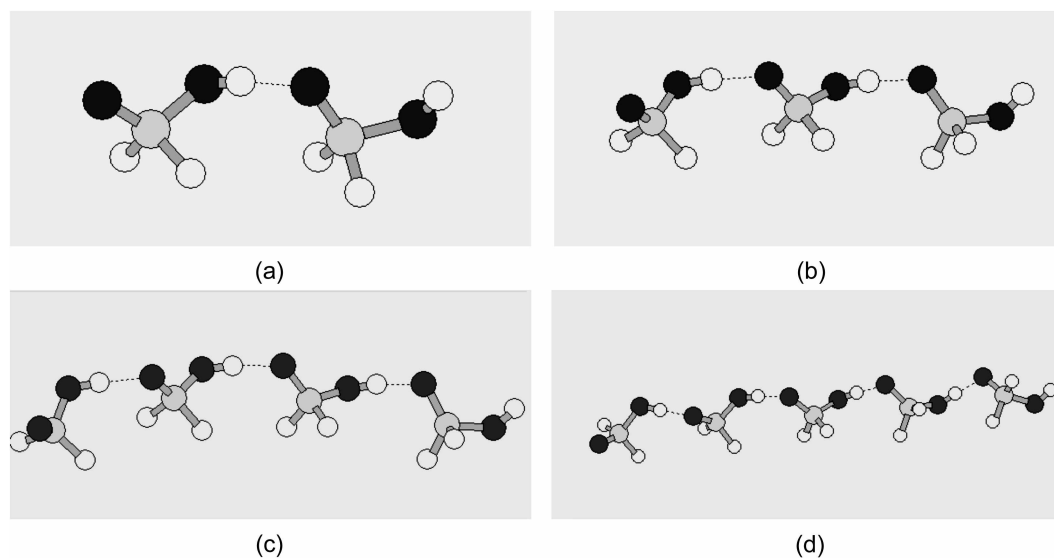


Fig. 8. The optimized structures of two, three, four and five member chain of the HPA.

Table 3 Optimized Parameters for central HPA unit (in Angstroms and Degrees)B3LYP/6-31G\*\*

Name	Mono-mer( $H_2PO_2$ )	Tri-mer ( $H_3P_3O_6$ )	Penta-mer ( $H_5P_5O_{10}$ )	Exp. Solid <sup>18</sup>
R(P-OH)	1.628	1.597	1.586	1.512
R(O-H)	0.969	0.994	1.004	1.22
R(P-H)	1.410	1.408	1.409	1.392
R(P-H)	1.416	1.417	1.415	1.392
R(P=O)	1.485	1.498	1.499	1.512
R(O-H...O)		2.66	2.601	2.44
A(POH)	111.9	117.2	118.9	-
A(HPO)	97.0	99.1	100.1	-
A(HPO)	103.6	104.6	104.9	-
A(OPO)	117.9	119.6	119.7	114.9
A(O-H...O)		172.7	175.0	-

The effects of increasing HPA chain units are reflected in Table 3. The dihedral angle, which is responsible for chain screwing changing about  $10^\circ$  (dimmer -128.83, trimer and -119.5, tetramer -108.5 and pentamer -101.3 degrees) P=O bond length, as expected, it is elongated about  $0.013 \text{ \AA}$  from monomer to trimer but the change from trimer to pentamer is small and equal to  $0.001 \text{ \AA}$  Table 3. The reported bond length<sup>18</sup> for both of the P-O bonds in the crystalline environment are the same and equal

to the  $1.512 \text{ \AA}$  (which is close to the calculated P=O bond length in free space) and the hydrogen bond is almost linear with a single minimum potential. The crystalline environment mainly is imposes on the P-OH and O-H bond lengths and equalizes them with related ones but the gas phase calculations predicts the HPA units keeping almost their monomer structure and connected to each other through a long hydrogen bonds.

The vibrational frequencies are calculated for

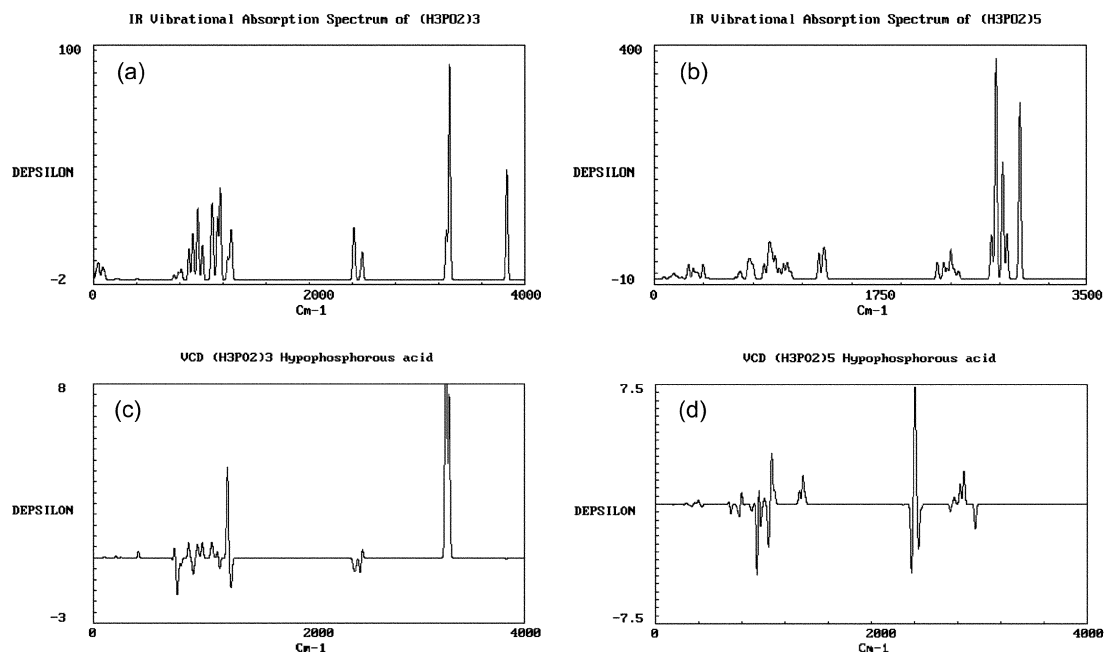


Fig. 9. IR (a, b) and VCD (c, d) absorption spectra of tri-and pentamers of the HPA.

HPA chains using the B3LYP/6-31G\*\* approach. Then the IR and VCD modeled spectra of these molecules are constructed and presented in Figs. (9-a, b, c, d). The superiority of VCD to IR is its analytical applications.

## CONCLUSION

A DFT/B3LYP/6-31G\*\* calculation is performed to optimize a series of HPA compounds in chains, determination of the potential energy surfaces, finding spatial isomeric pathway, computation of single bond potential energy, calculations of IR, and vibrational circular dichroism spectra using Gaussian 98w package.

Our PES calculations confirm two mirror stable conformations of the HPA with  $C_1$  symmetry. The PES can be considered to consist of the many

Morse type potentials with varying depth separated on a three dimensional space whose approaching to infinity sides are aligned to the P-O bond axis. The variation method calculations, which are generated by us, used to determine tunneling between two isomeric conformations, vibrational energy levels, transitions and probabilities are done with it.

The HPA chain in free space screw itself by about  $10^\circ$  for each unit. IR and VCD spectra are constructed for mono-, tri- and penta-mer of the HPA to approach to the solid state spectra. And it is found that by increasing number HPA units in the chain it is possible to approach to the solid state spectra, Table 4 and Fig. 10. In Fig. 10 the variation of the OP(OH) bend ( $\nu_2=394\text{ cm}^{-1}$ ) and P-(OH) stretch ( $\nu_4=1015\text{ cm}^{-1}$ ) with the number of HPA unites are shown and clearly supporting our theoretical calculations.

Table 4 Assignments of the calculated frequencies (with B3LYP/6-31G\*\* in  $\text{cm}^{-1}$ ) of Mono-, Tri-, Penta-mers of the HPA, which are compared with solid state spectra.

Expt.[8]	Penta	Tri	Mono	Assignment
232	231.5	226.7	237.5	OP(OH) torsion
394	398.3	406.9	413.3	OP (OH) bend+OH torsion
805	784.8	775.3	785.1	PH <sub>2</sub> rock-POH bend
1015	955.3	929.3	859.7	P-(OH) stretch
928	929.3	922.0	898.2	PH <sub>2</sub> twist
11300	1011.7	971.0	1028.1	POH bend-HPO bend
1098	1105.8	1106.6	1117.1	PH <sub>2</sub> wag+POH bend
1122	1145.4	1148.0	1165.0	PH <sub>2</sub> scissor+P=O stretch
1260	1260.6	1265.6	1296.6	PH <sub>2</sub> scissor+P=H stretch
2442	2435.0	2421.4	2427.1	PH asym. stretch
2465	2484.4	2487.0	2474.2	PH sym. stretch
1100	3092.4	3273.0	3817.1	OH stretch

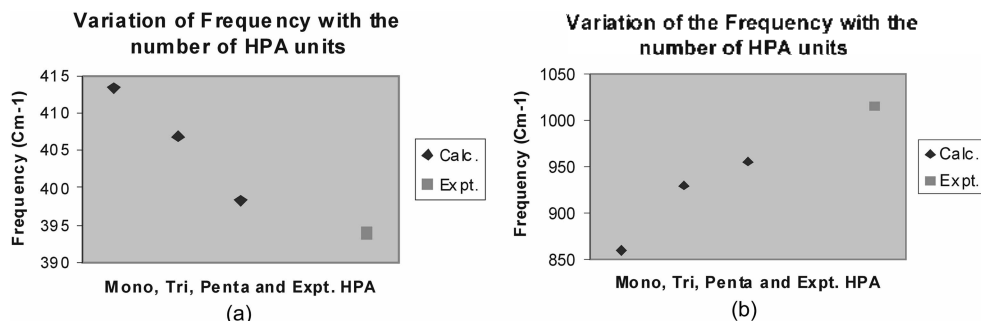


Fig. 10: a: the variation of the OP(OH) bend ( $\nu_2=394\text{ cm}^{-1}$ ) and b: P-(OH) stretch ( $\nu_4=1015\text{ cm}^{-1}$ ) with the number of HPA unites in the chain with corresponding experimental values.



Inspection of the Table 4 more closely indicate that, in general, the vibrational frequencies with increasing of the HPA units except for POH bend at  $11300\text{ cm}^{-1}$  and OH stretch at  $1100\text{ cm}^{-1}$  are improved. The reason may be arises from the point that we let the chain to optimize freely in the space. The crystalline environment imposes to the HPA units to appear in different optimization.

To show the trends of frequency optimization  $\nu_2$  and  $\nu_1$  as an examples are plotted in Fig. 10 for visual demonstration.

## REFERENCES

1. D. E. C. Corbridge: *phosphorous: An Outline of its Chemistry, Biochemistry, and Technology*, Amsterdam: Elsevier Science Publishing Co., 3<sup>rd</sup> ed., New York (1985).
2. E. L. Stewart, N. Nevins, N. L. Allinger, and J. P. Bowen, *J. Org. Chem.* **1997**, *62*, 5198. E. L. Stewart, N. Nevins, N. L. Allinger, and J. P. Bowen, *J. Org. Chem.* **1999**, *64*, 5350.
3. J. M. Williams and S. W. Peterson, *Spectrosc. Inorg. Chem.*, **1971**, *2*, 1.
4. D. Hadzi, B. Orel and A. Novak, *Spectrochim. Acta. Part A*, **1973**, *29*, 1745.
5. D. Hadzi, M. Obradovic, B. Orel and T. Solmajer, *J. Mol. Struct.*, **1972**, *14*, 439.
6. L. Angeloni, M. P. Marzocchi, D. Hadzi, B. Orel and G. Sbrana, *Chem. Phys. Lett.*, **1974**, *28*, 201.
7. L. Angeloni, M. P. Marzocchi, D. Hadzi, B. Orel and G. Sbrana, to be published.
8. S. Detoni, D. Dadzi and B. Orel, *Journal of Molecular Structure*, **1976**, *33*, 279.
9. <http://www.rhodium.ws/chemistry/hypophosphorous.html>
10. M. J. Frisch, G. W. Trucks, H. B. Schlegel, G. E. Scuseria, M. A. Robb, J. R. Cheeseman, V. G. Zakrzewski, J. A. Montgomery, Jr., R. E. Stratmann, J. C. Burant, S. Dapprich, J. M. Millam, A. D. Daniels, K. N. Kudin, M. C. Strain, O. Farkas, J. Tomasi, V. Barone, M. Cossi, R. Cammi, B. Mennucci, C. Pomelli, C. Adamo, S. Clifford, J. Ochterski, G. A. Petersson, P. Y. Ayala, Q. Cui, K. Morokuma, D. K. Malick, A. D. Rabuck, K. Raghavachari, J. B. Foresman, J. Cioslowski, J. V. Ortiz, A. G. Baboul, B. B. Stefanov, G. Liu, A. Liashenko, P. Piskorz, I. Komaromi, R. Gomperts, R. L. Martin, D. J. Fox, T. Keith, M. A. Al-Laham, C. Y. Peng, A. Nanayakkara, C. Gonzalez, M. Challacombe, P. M. W. Gill, B. Johnson, W. Chen, M. W. Wong, J. L. Andres, C. Gonzalez, M. Head-Gordon, E. S. Replogle, and J. A. Pople, Gaussian, Inc., Pittsburgh PA, 1998.
11. A. C. C. J. Roothan, "New Developments in Molecular Orbital Theory," *Rev. Mod. Phys.* **1951**, *23*, 69. B. J. A. Pople and R. K. Nesbet, "Self-Consistent Orbitals for Radicals," *J. Chem. Phys.* **1954**, *22*, 571. C. R. McWeeny and G. Dierksen, *J. Chem. Phys.* **1968**, *49*, 4852.
12. M. Head-Gordon, J. A. Pople and M. J. Frisch, *Chem. Phys. Lett.* **1988**, *153*, 503. A. M. J. Frisch, M. Head-Gordon and J. A. Pople, *Chem. Phys. Lett.* **1990**, *166*, 275. B. M. J. Frisch, M. Head-Gordon and J. A. Pople, *Chem. Phys. Lett.* **1990**, *166*, 281. C. M. Head-Gordon and T. Head-Gordon, "Analytic MP2 Frequencies Without Fifth Order Storage: Theory and Application to Bifurcated Hydrogen Bonds in the Water Hexamer," *Chem. Phys. Lett.* **1994**, *220*, 122. D. G. W. Trucks, M. J. Frisch, J. L. Andres and H. B. Schlegel, "An Efficient Theory and Implementation of MP2 Second Derivatives," in prep. (1998). J. A. Pople, R. Krishnan, H. B. Schlegel and J. S. Binkley, "Electron Correlation Theories and Their Application to the Study of Simple Reaction Potential Surfaces," *Int. J. Quant. Chem.* **XIV**, 545 (1978).
13. A. C. Lee, W. Yang and R. G. Parr, "Development of the Colle-Salvetti correlation-energy formula into a functional of the electron density," *Physical Review B*, **1988**, *37*, 785. B. A. D. Becke, *Phys. Rev. A* **1988**, *38*, 3098. C. B. Miehlich, A. Savin, H. Stoll and H. Preuss, *Chem. Phys. Lett.* **1989**, *157*, 200. D. A. D. Becke, "Density-functional thermo chemistry III The role of exact exchange," *J. Chem. Phys.* **1993**, *98*, 5648.
14. HyperChem 7.0, molecular modeling system, Hypercube, Inc (2002).
15. J. R. Cheeseman, M. J. Frisch, F. J. Devlin and P. J. Stephens, "Ab Initio Calculation of Atomic Axial Tensors and Vibrational Rotational Strengths Using Density Functional Theory," *Chem. Phys. Lett.* **1996**, *252*, 211.
16. Surfer version 7.02, Golden software, Inc (2000), Colorado 80401-1866.
17. R. L. Somorjai and D. F. Hornig, *J. Chemical physics*, **1962**, *36*, 1980.
18. J. M. Williams: Ph. D. Thesis, Washington state University (1966).